Environmental Science & Technology

Article

pubs.acs.org/est

Chemical and Isotopic Thresholds in Charring: Implications for the Interpretation of Charcoal Mass and Isotopic Data

Lacey A. Pyle,*[,†] William C. Hockaday,[‡] Thomas Boutton,[§] Kyriacos Zygourakis,[∥] Timothy J. Kinney,[†] and Caroline A. Masiello[†]

[†]Department of Earth Science, Rice University, 6100 Main St MS 126, Houston, Texas 77005, United States

[‡]Department of Geology, Baylor University, One Bear Place #97354, Waco, Texas 76798, United States

[§]Department of Ecosystem Science and Management, Texas A&M University, 2138 TAMU, College Station, Texas 77843, United States

[∥]Department of Chemical and Biomolecular Engineering, Rice University, 6100 Main St MS-362, Houston, Texas 77005, United States

Supporting Information

ABSTRACT: Charcoal plays a significant role in the long-term carbon cycle, and its use as a soil amendment is promoted as a C sequestration strategy (biochar). One challenge in this research area is understanding the heterogeneity of charcoal properties. Although the maximum reaction temperature is often used as a gauge of pyrolysis conditions, pyrolysis duration also changes charcoal physicochemical qualities. Here, we introduce a formal definition of charring intensity (CI) to more accurately characterize pyrolysis, and we document variation in charcoal chemical properties with variation in CI. We find two types of responses to CI: either linear or threshold relationships. Mass yield decreases linearly with CI, while a threshold exists across which % C, % N, and δ^{15}N exhibit large changes. This CI threshold co-occurs with an increase in charcoal aromaticity. C isotopes do not change from original biomass values, supporting the use of charcoal δ^{13}C signatures to infer paleoecological conditions. Fractionation of N isotopes indicates that fire may be enriching soils in ^{15}N through pyrolytic N isotope fractionation. This influx of "black N" could have a significant impact on soil N isotopes, which we show theoretically using a simple mass-balance model.

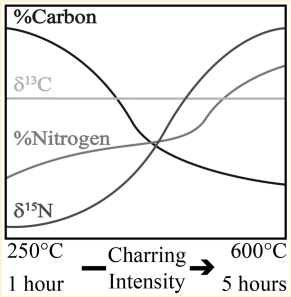

INTRODUCTION

Black carbon is the range of products that results from incomplete combustion,[1−3] and this continuum can be quite diverse. One form of anthropogenically produced material on this spectrum, biochar (which is produced under restricted O_2), has the potential to help address several environmental issues, dependent on biochar quality; for instance, biochar can promote soil fertility and plant growth,[4] and sequester carbon[5−7] to variable degrees dependent on pyrolysis conditions. Another form, wildfire charcoal (which is produced under a range of O_2 concentrations and substrate sizes) is ubiquitous in soils[8] and sediments,[9] is often older than bulk organic carbon, and can provide fire-event markers. However, the range of charcoal properties is large, causing complications in optimizing biochar for soil remediation and carbon sequestration and in using charcoal to reconstruct past fire regimes.

Charcoal chemical properties undoubtedly change with increasing pyrolysis temperatures. Carbon (C) and nitrogen (N) isotopes and chemical functionalities show stark changes during pyrolysis (e.g., refs 6, 10−12, and others). An increase in aromatic C functionalities with increasing maximum pyrolysis temperature is well-established,[10,12−14] as well as a decrease in aliphatic and polysaccharide functionalities. However, C isotopes have been shown to stay relatively unchanged under differing pyrolysis conditions,[13,15] contributing to the use of charcoal C isotopes in paleoecological studies. N in charcoal, or black N, is far less studied due to its lower concentrations, yet black N also undergoes chemical changes during pyrolysis, forming heterocyclic N functionalities not present in the original biomass.[16−18] N isotopes, however, seem to undergo very little change during the charring process,[19−21] as is seen with C isotopes, yet the studies that observe ^{15}N through pyrolysis have not covered a large range of conditions. In natural fires with higher temperatures, increases in δ^{15}N in the environment have been observed,[22] which could be due to the fractionation of black N during charring.

Increasing pyrolysis duration also results in similar changes in charcoal properties as increasing maximum pyrolysis temperature.[23−28] Despite this, maximum pyrolysis temperature is often used alone as a measure of overall pyrolysis conditions.[23−26] The conflation of temperature and reaction duration may at least partially explain the differences in properties between charcoals produced under apparently similar conditions. By holding the maximum temperature

Received: June 25, 2015
Revised: October 26, 2015
Accepted: November 2, 2015
Published: November 2, 2015

DOI: 10.1021/acs.est.5b03087
Environ. Sci. Technol. 2015, 49, 14057−14064

constant and only varying the duration of pyrolysis, early experiments showed that charcoals produced over a longer duration had greater surface area and aromaticity and an increased capacity for pollutant sorption,[29] trends also found with increasing maximum pyrolysis temperature.[30] In studies where the effects of both maximum temperature and treatment duration were measured concurrently, increases in both pyrolysis conditions resulted in greater surface area (as measured with BET surface area analysis); greater ash content; more relative amounts of N, potassium, and phosphorus; greater C-to-H ratios; lower yields; lower C-to-N ratios; and lower amounts of volatile matter.[23−26] Additionally, the higher heating value (as measured with bomb calorimetry) and amount of fixed C both increased independently with temperature and treatment duration.[25] This may explain why soil incubation experiments have displayed a concurrent increase in lifetime of applied charcoals with increases in both treatment duration and temperature,[23,25,31] as well as less mineralized charcoal C and greater amounts of energy required to oxidize charcoal C,[25,27] either biotically or abiotically.[28] Many studies have noted that the charring duration results in chemical differences in charred products, but this connection is not typically incorporated into broader conclusions.[27]

In this study, we introduce a metric that combines the temperature and duration of pyrolysis to characterize the continuum of chemical transformations observed as biomass is pyrolyzed. Although there are many other parameters that can be varied in pyrolysis reactors (e.g., sample insulation, O_2 concentration in purge gas, and particle size), here we focus on maximum pyrolysis temperature because it is widely used to characterize charcoal and is often the only measure of reaction conditions. This is a formalization of the concept of charring intensity (CI) introduced previously,[2,32] intended to better represent the charring process in pyrolysis reactors at thermal equilibrium.

We tested the effectiveness of this new metric at representing data for a series of charcoals made from a range of feedstocks. Because the metric of CI presented here is designed to better capture chemical changes occurring throughout the charring process, we hypothesized that it may provide a better intercomparison method between charcoals. To test this, we analyzed the samples for chemical and isotopic qualities across a large gradient of CI values. Our results reveal chemical trends resulting from the temperature and duration of charring and also have implications for soil N cycling, in which the periodic influx of black N may cause a modest increase in the δ^{15}N of soils in fire-prone ecosystems. To test this hypothesis, we added a fire component to a simple mass-balance model of nitrogen isotopic and mass fluxes in soils and plants and found that even modest charcoal N contributions can have a large impact on soil N isotopic composition.

■ MATERIALS AND METHODS

Biomass Samples. We examined the effects of CI on charcoal properties using charcoal produced from a suite of four feedstocks: applewood (*Malus domestica*), mesquite wood (*Prosopis glandulosa*), cocklebur (*Xanthium strumarium*), and corn stover (*Zea mays*). We chose these to represent wood, grass, and herbaceous materials and to span a range of C and N isotopic signatures. All of the samples were first dried in an oven at 120 °C for 24 h and then ground using a Thomas Scientific Wiley Mini Mill 3383-L10 to pass a 841 μm sieve.

Charcoal Production. After grinding the samples, we made pellets of all of the samples using a press (Parr 2811). We put five pellets (∼1 g) of each biomass sample in ceramic crucibles and covered them with a fine silica powder (U.S. Silica Company Min-u-sil-40) up to 5 mm below the top of the crucible to minimize oxygen exposure during pyrolysis. This silica is 99.5% SiO_2 and has a pH of 6.5. All of the particles have an equivalent spherical diameter less than 50 μm, and 50% are less than 10 μm.[33] Although this was an efficient method for oxygen restriction, some silica may have adhered to our samples, introducing silica peaks in the FTIR spectra and depressing the %C in the chemical analyses. We fired the crucibles in a muffle furnace over a range of temperatures and times, from 250 to 600 °C and from 1 to 5 h at 5 °C s^{-1}, and massed all sample-containing crucibles before and after pyrolysis to find mass yields. At higher temperatures, the samples did not survive 5 h reactions, limiting data from this end of the CI spectrum.

Integral Metric of Charring Intensity. Previously, charring intensity has been used as a nonquantitative representation of the amount of energy input to biomass during pyrolysis, roughly understood to be related to the maximum pyrolysis temperature. However, we argue here that the continuum of charring products versus temperature[2] can be better represented by an equation integrating the heat applied and the reaction duration. Here, we define CI as the integral:

$$\mathrm{CI} = \int_{t_0}^{t_f} T(t)\,\mathrm{d}t$$

where $T(t)$ is the temperature history of the pyrolyzing biomass. For the typical slow pyrolysis experiment, biomass is heated to a maximum temperature T_{max}, held there for some time, and then allowed to cool. We define the beginning temperature of charring as 200 °C, below which dehydration is the main reaction and above which changes to the chemical C structure may start occurring.[6,34,35] Therefore, the limits of integration t_0 and t_f are defined as the times at which the sample temperature rises above 200 °C during the heating phase and drops below 200 °C during the cooldown phase.

To quantify the CI for each sample, we inserted a thermocouple in the biomass and recorded the temperature of the pyrolyzing sample at 10 s intervals. After noting the time level N, at which the temperature first reached 200 °C ($T_N \approx 200°C$), and the time level M, at which the temperature dropped back to 200 °C ($T_M \approx 200°C$), we calculated the integral by summing all the temperatures between these two points and multiplying the sum by the measurement time interval:

$$\mathrm{CI} = \left(\sum_{i=N}^{M} T_i\right)\cdot \Delta t$$

Elemental Analysis and Isotope Measurements. We measured sample % C, % N, and % H on a Costech ECS 4010 CHNSO Analyzer at Rice University. Isotopic measurements were performed in the Stable Isotopes for Biosphere Sciences Lab at Texas A&M University. Both charred and uncharred plant materials were pulverized, weighed into tin capsules using a microbalance, and analyzed for elemental (C and N) and isotopic (δ^{13}C and δ^{15}N) composition using a Carlo Erba EA-1108 (CE Elantech, Lakewood, NJ) elemental analyzer interfaced with a Delta Plus (ThermoFinnigan, San Jose, CA)

DOI: 10.1021/acs.est.5b03087
Environ. Sci. Technol. 2015, 49, 14057−14064

isotope ratio mass spectrometer operating in continuous flow mode. C and N isotope ratios are presented in δ notation:

$$\delta = [(R_{sample} - R_{std})/R_{std}] \times 10^3$$

where R_{sample} is the $^{13}C/^{12}C$ or $^{15}N/^{14}N$ ratio of the sample, and R_{std} is the $^{13}C/^{12}C$ or $^{15}N/^{14}N$ ratio of the standard. $\delta^{13}C$ values were expressed relative to the V-PDB standard,[36] and $\delta^{15}N$ values were expressed relative to the atmospheric N standard.[37] Precision of duplicate measurements was <0.1 ‰ for $\delta^{13}C$ and <0.2 ‰ for $\delta^{15}N$.

Fourier Transform Infrared Spectrometry. We generated attenuated total reflectance Fourier transform infrared (ATR-FTIR) spectra using a Nexus 670 Fourier transform infrared spectrometer (Thermo Scientific, Waltham, MA). Prior to analysis, we ground the samples and dehydrated each sample in an oven overnight at 120 °C to reduce the signal from adsorbed water. We then made measurements on three separate aliquots of each sample. We baseline-corrected each spectrum, analyzed the peak areas using Fityk 0.9.8 software,[38] and present results as percent radiation transmitted. The peak areas are solved for in Fityk with a Gaussian function, and peak areas were then averaged between the three subsamples before being used for analysis.

Mass-Balance Model. We used a simple mass-balance model for N ecosystem modeling outlined in a grassland study[39] for total soil N (N_s) and plant N (N_p) as well as isotope ratios:

$$\frac{dN_s}{dt} = I_{ex} - k_{ex}N_s + k_sN_p - k_pN_s$$

$$\frac{dN_p}{dt} = k_pN_s - k_sN_p + I_{fix}$$

$$\frac{d15N_s}{dt} = I_{ex}R_{ex} - k_{ex}\alpha_{ex}15N_s + k_s15N_p - k_p\alpha_p15N_s$$

$$\frac{d15N_p}{dt} = k_p\alpha_pR_sN_s - k_s15N_p + I_{fix}R_{fix}$$

where N is total N, ^{15}N is total amount of the heavy isotope of N, I_{ex} is N deposition (kg m^{-2} yr^{-1}), I_{fix} is N fixation (kg m^{-2} yr^{-1}), k is the decay constant for N reservoirs (yr^{-1}), R is the ratio of ^{15}N to ^{14}N for N reservoirs, and α is the fractionation factor between reservoirs.[39] Subscripts s and p refer to soil and plant pools, while subscript "ex" refers to N deposition and "fix" refers to N fixation. We extended the model using Matlab software by adding a periodic fire pulse where a large portion of the plant N reservoir is lost to the atmosphere and a smaller portion is transferred to the soil reservoir with the associated fractionation factor for charring we found in our results. The parameters for the extended model are in Supplemental Tables 2 and 3.

RESULTS AND DISCUSSION

Here, we compare the effectiveness of CI at characterizing charcoal properties to that of peak temperature alone and find that CI is a better metric. We also find that some properties of charcoal, such as mass yield, have a linear relationship with CI, while others (%N, $\delta^{15}N$, %C) display a step-function relationship. These step-function relationships share a common threshold value for CI, which is the boundary between more heterogeneous charcoals and more aromatically condensed charcoals. Additionally, we find that N isotopes fractionate with increasing CI while C isotopes did not, which has implications for soil, paleoecological, and archeological studies.

Charring Intensity Linearly Captures Mass Yield. CI better captures mass changes during pyrolysis compared to peak temperature alone (Figure 1A,B). The linear regression

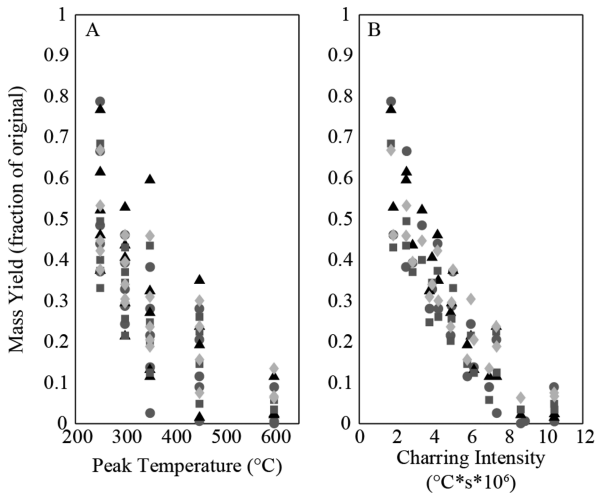

Figure 1. Pyrolyzed charcoal mass yields compared to (A) temperature and (B) charring intensity. Apple char samples are represented by circles, corn char by squares, cocklebur char by diamonds, and mesquite char by triangles.

for mass loss improves from an R^2 range of 0.54−0.64, when mass versus temperatures were compared, to an R^2 value of 0.74−0.84, when comparisons were made of mass versus CI across all types of biomass. Holding temperature constant and varying only reaction duration (temperature isolines in Figure 1A) shows that charring transformations continue for the entire duration of reaction rather than ceasing when the highest temperature is reached. This impact on trends is also observed in the other chemical characteristics we measured (Supplementary Figures 1 and 2).

Chemical Thresholds in Charring: % C, $\delta^{13}C$, % N, and $\delta^{15}N$. Unlike mass yield, %C shows evidence of a chemical threshold in the pyrolysis process occurring at a CI of ∼5.0 × 10^6 °C·s. All four plant materials show a marked increase in C loss above this threshold CI (Figure 2), although % C decreased more in the herbaceous plants (corn and cocklebur) than it did in the woody material (apple and mesquite). The apple and mesquite wood chars used in this study decrease from average % C values of ∼63% at low CI to ∼51% at higher CI values. Corn stover and cocklebur chars both have average % C values of approximately 52%, decreasing at high CI to % C values as low as 2.3% for corn stover and 4.5% for cocklebur. The much greater C loss in the corn stover and cocklebur is likely due to the lower levels of lignin in these plant precursors,[40] which breaks down at higher intensities than cellulose and hemicellulose.[2,35] There may also have been a contribution from silica, depressing the % C in the corn and cocklebur, while the much higher values in the hardwoods are due to preferential preservation; this preservation allowed easier picking of the samples from the crucible and, hence, a lower chance of silica contamination.

In spite of these large C losses, $\delta^{13}C$ values are not significantly altered in any of the plant materials across all CI values (Figure 3). These data are in agreement with most other

DOI: 10.1021/acs.est.5b03087
Environ. Sci. Technol. 2015, 49, 14057−14064

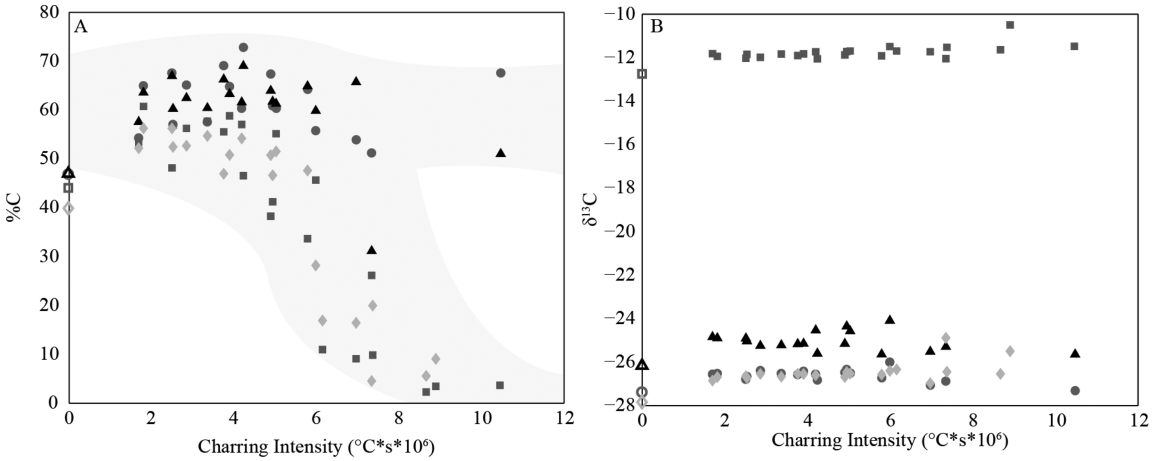

Figure 2. (A) Percent carbon of original biomass remaining in pyrolyzed samples. (B) Carbon isotope values of pyrolyzed samples. Hollow symbols on the *y*-axis are uncharred biomass values. Apple char samples are represented by circles, corn char by squares, cocklebur char by diamonds, and mesquite char by triangles.

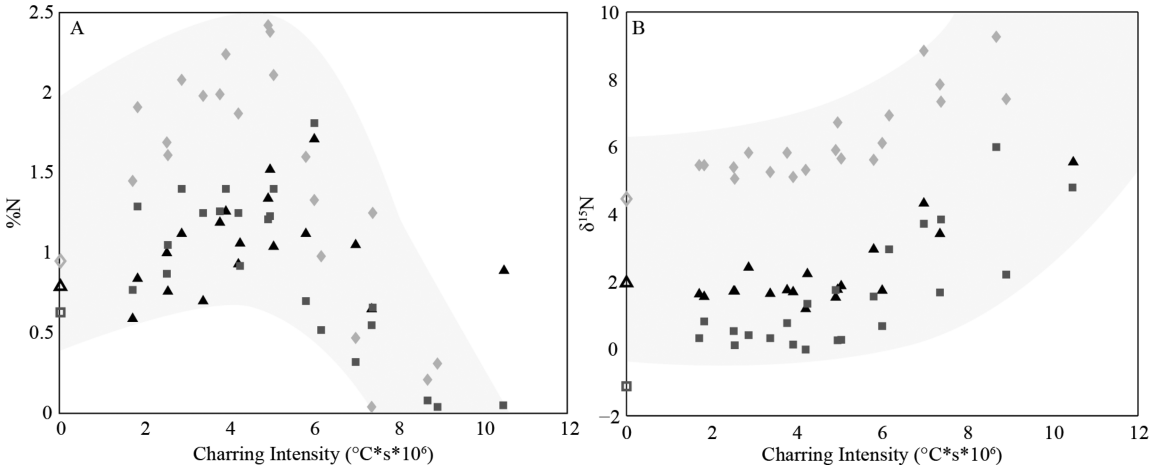

Figure 3. (A) Percent nitrogen of the original biomass in the remaining pyrolyzed material. (B) Nitrogen isotope values of each pyrolyzed sample. Hollow symbols on the *y*-axis are uncharred biomass values. Corn char samples are represented by squares, cocklebur char by diamonds, and mesquite char by triangles. (For apple char, very low initial N concentrations limited detection of changes in % N, and it is excluded from N figures.).

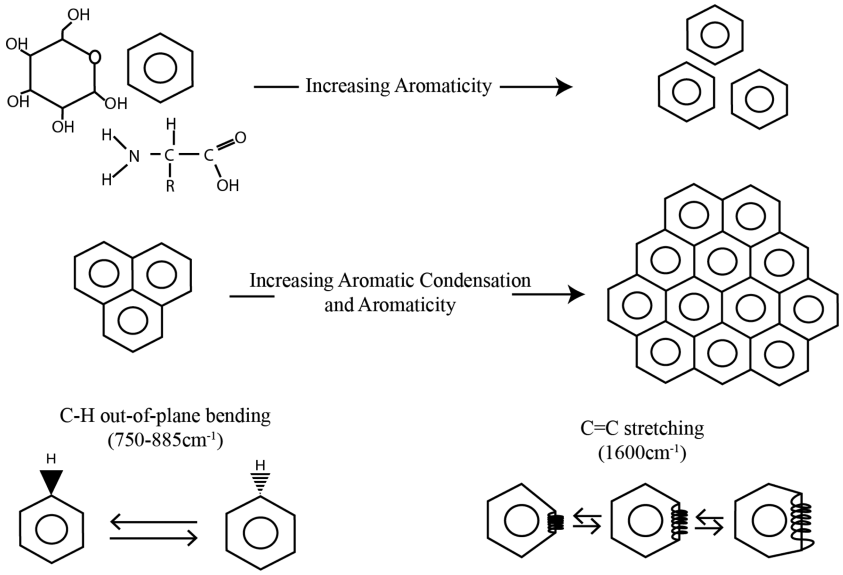

Figure 4. Diagram of the chemical vibrations observed when measuring the degree of charring. As charring progresses, aromatic condensation increases, resulting in bigger and more rigid sheets where C═C stretching is limited.

DOI: 10.1021/acs.est.5b03087
Environ. Sci. Technol. 2015, 49, 14057−14064

isotopic studies of charcoal formation, where on average, the total fractionation observed from biomass values is generally <1−2‰[15] (higher fractionations can occur within the aromatic fraction but at much greater temperatures[41] and when combustion is the dominant reaction[42]). Our results support the efficacy of using charcoal δ^{13}C as a proxy to reconstruct paleoclimate[43,44] and prehistoric human diets.[21]

The changes in charcoal % N with CI are due to the chemical transformation of N compounds followed by their volatilization. There is an initial increase in % N across all feedstocks as CI increases (Figure 4). The % N early in the charring process ranged from 0.6 to 1.8% and then rose to maximum values of 1.1 to 2.4% as CI increased to the threshold value of 5.0×10^6 °C·s (Figure 4). The increase in % N is likely due to the preferential volatilization of reactive C and O, while N-containing compounds are initially transformed into more stable heterocyclic and aromatic compounds. Previous studies have shown increases in CI converting less-stable N functionalities into pyrrolic and then pyridinic N, until N-containing heterocyclic compounds made up the majority of the N still present,[16−18,45] a process even more prevalent in grasses than woods.[18,46] The threshold for this switch from transformation of N functional groups to the decomposition of the more stable aromatic N occurs around the same CI for all species, approximately 5.0×10^6 °C·s, after which all charcoal species begin showing decreases in %N (Figure 3).

At low CI, there is very little N fractionation, while at higher CI values, δ^{15}N increases significantly. This effect shows up for all feedstocks with a measurable % N. The charcoal δ^{15}N also displays a threshold effect, with significant fractionation from original biomass after the 5.0×10^6 °C·s threshold in the CI is crossed (Figure 3). Before this charring threshold is reached, mesquite wood, corn stover, and cocklebur charcoals have average isotopic values of 1.7 ± 0.3‰, 0.4 ± 0.3‰, and 5.4 ± 0.3‰, respectively (the initial δ ^{15}N values of mesquite (1.9‰) and corn stover (−1.1‰) are different from cocklebur (4.4‰), likely due to the fact that corn was grown with fertilizer, and mesquite is a legume that fixes atmospheric N_2 symbiotically. Thus, corn and mesquite have δ ^{15}N values close to the 0‰ value of atmospheric N_2.[47] After the threshold is crossed, there is significant isotopic fractionation, resulting in δ^{15}N values of 5.5−9.3‰ at the highest CI. This is an isotopic shift of 3.9−5.6‰. This pattern supports the interpretation that initially most N functionalities are transformed to stable heterocyclic rings before those, too, are decomposed at higher intensities, resulting in isotopic and mass fractionation after the threshold CI has been reached. Another interpretation of the fractionation is that during pyrolysis, nitrate is formed and enriched in ^{15}N, and the ratio of ash nitrate to black N increases with CI. Our method does not differentiate between black N and ash N, but in either case, charring will result in an import of isotopically enriched N to soils. This enrichment in δ^{15}N with charring may have the potential to influence N isotope ratios in the surface soils of fire-prone ecosystems (see the Implications for Interpreting Soil δ15N Data section).

FTIR Shows Chemical Trends along Charring Intensity Gradient. We evaluate three FTIR peak ratios to probe the nature of the chemical shift occurring at CI values of 5.0×10^6 °C·s, focusing on previously cited peak ratios that are indicative of the degree of charring (1620 cm^{-1}:1700 cm^{-1}) and degree of condensation (aromatic peaks between 885 and 750 cm^{-1}:1600 cm^{-1}).[2,48−50] Degree of charring is often represented as the ratio of C═C to C═O stretching adsorption bonds.[48,51] Although both peaks increase in the early stages of charring, the peak at 1700 cm^{-1} (C═O) begins to disappear as oxygen is lost at higher charring intensities; thus, higher ratios indicate greater charring[48,51] and are a measure of sample aromaticity (fraction aromatic C in a sample).[10] Degree of condensation is the ratio of aromatic C−H out-of-plane-bending to C═C aromatic stretching bonds and increases in this ratio indicate a transition to larger, more rigid sheets of connected aromatic rings[2,50] or an increase in aromatic condensation.[10,12] Increases in degree of charring are indicative of the creation of more aromatic C rings relative to other functional groups, while increases in degree of condensation correspond to larger aromatic sheets forming (Figure 4).

The representation of the increase in degree of condensation by an *increase* in the ratio of C−H aromatic bonds to C═C bonds is nonintuitive because there are relatively more inner C═C bonds than outer C−H bonds in larger aromatic sheets. For example, a single aromatic ring has six C−H bonds and three C═C bonds, while a three-ring sheet has nine C−H bonds and nine C═C bonds. However, this ratio increase reflects the signals from these bonds, not their absolute amounts. As the rigidity of larger aromatic sheets increases, they are less able to stretch (and generate signal): C═C within large, rigid aromatic sheets generates a reduced signal even though more double bonds are present than C−H bonds (Figure 4).[2,50] Degree of charring and degree of condensation increase similarly with CI, although the trend is more pronounced for the grass and herbaceous dicot than it is for the two woods. Changes in the charcoal FTIR spectra across the CI gradient show a loss of the original biomass complexity as charcoals progress to larger, more rigid aromatic structures.

Integrated Chemical and Isotopic Changes during Pyrolysis. We use the FTIR peak ratios discussed above to examine the chemical changes occurring across our charring continuum and explore the relationship between the threshold behavior in the N isotopes and the overall chemical structure of the charcoal. The degree of charring begins increasing at low CI and continues through the highest values as molecules are progressively transformed into stable aromatic rings. However, the increase in the peak ratio indicative of degree of condensation exhibits threshold behavior with little change before 5.0×10^6 °C·s and larger changes after. The threshold pattern observed in N composition and isotopes as well as the degree of condensation peak ratios may indicate that although N compounds are being transformed into aromatic N-containing compounds, these heterocyclic compounds are not incorporated into larger condensed aromatic sheets. When the threshold is reached, therefore, heterocyclic-N compounds are pyrolyzed and lost.

Implications for Interpreting Soil δ^{15}N Data. Many different N transformations and losses can lead to a relative enrichment in ecosystem ^{15}N, with variable magnitudes,[52] but the addition of pyrogenic matter complicates this picture. In ecological fire studies, an immediate postfire increase in δ^{15}N of plant N is widely observed (e.g., refs 22, 53, and 54). Several theories exist as to why this happens, including consumption of low δ^{15}N surface litter during fire, forcing plants to obtain N from deeper δ^{15}N-enriched soil N stores[52] and increased nitrification postfire, leaving behind a δ^{15}N-enriched ammonium pool.[22,54] However, a recent paper proposed that the addition to the soil pool of fire-altered materials enriched in ^{15}N is actually the most important fire effect.[22] Previous studies have shown very little fractionation in black N, yet these studies

DOI: 10.1021/acs.est.5b03087
Environ. Sci. Technol. 2015, 49, 14057−14064

used much lower temperatures and durations than this study.[19−21] In natural ecosystems where temperatures are often greater than 250 °C and durations longer than 1 h,[55] fires are likely to cause an increase in both whole-soil and charcoal δ^{15}N isotopes.[22,56]

N in charcoal has been ignored as a contributor to the soil N cycle because N is usually <5% charcoal by mass, but new evidence suggests that black N may play a more complex role in the soil N cycle.[57,58] Our results indicate that above the CI threshold of 5.0×10^6 °C·s, N does begin to fractionate with ^{14}N in pyrolyzed biomass being preferentially lost because pyrolysis discriminates against the heavy isotope. In natural fires, pyrolysis in the interior of substrates likely competes with combustion at the surface of biomass particles where O_2 is readily supplied,[59] potentially resulting in a dominance of pyrolysis type reactions in woody materials and a dominance of combustion-type reactions in grasslike materials.[55] Therefore, hotter, longer forest fires will result in greater fractionation and an input of high δ^{15}N substrate to the top of the soil column, while grassland fires may have a lower influence from pyrolysis. δ^{15}N values tend to increase with depth, which in the past has been explained by age-dependent N fractionation patterns or the addition of ^{15}N-depleted plant litter at the surface and ^{15}N-enriched mycorrhizal fungi tissues at depth.[47,52,60−62] After crossing the CI threshold, pyrogenic N additions to the topsoil are both stable and enriched in ^{15}N relative to their precursor organic matter, providing an additional potential mechanism that would result in older, deeper soil nitrogen having higher δ^{15}N values.

To examine the impact of fire-derived, δ^{15}N enriched charcoal on soil ^{15}N signatures in fire-prone ecosystems, we revised a simple model developed by Brenner et al. (2001) to simulate a fire event every 50 years in a grassland and every 100 years in a boreal forest. We estimate conservative fractionation factors on the basis of CI values reasonably expected in wild fires (approximately equivalent to 350 °C for 5 h, 450 °C for 4 h, or 600 °C for 3 h) and on the basis of the relative importance of pyrolysis that we would expect in a forest versus a grassland[63,64] (see Supplemental Tables 3 and 4), and we also estimate gaseous losses from combustion for the above-ground component.[65−67] We use MATLAB software to numerically simulate periodic fires for 4000 years to the steady-state and find that compared to model results without fire, a fire-moderated ecosystem had 2‰ higher δ^{15}N steady-state values in both the biomass and the soil, which we treat in this simple experiment as one pool (Supplemental Figures 4 and 5). This effect would likely become more pronounced in a model that included multiple depths and organic matter pools because black N may be more stable than other forms.[68] However, we caution that most of this shift is due to the atmospheric losses of above-ground biomass; still, approximately 25% of this shift was due to char N addition alone in our conservative simulations. This indicates that black N, when present, may shift soil N isotope profiles. These results mean that in ecosystems where fires persist for hours or burn hot, the use of N isotopes to reconstruct ecosystem δ^{15}N values requires careful evaluation.

The concept of CI presented here is a first step in standardizing comparisons between charcoals produced under different environmental conditions or in different laboratories, and our chemical data demonstrate that the previously observed importance of temperature in controlling charcoal qualities is better captured by total energy input. Our lab results also have implications for the interpretation of soil isotopic values, and our modeling experiment shows that black N may influence N soil dynamics, altering both SOM recalcitrance and soil δ^{15}N values. Thermal history impacts on charcoal qualities may also complicate reconstruction of past fire regimes because natural fires contain both fast-burning high-temperature regions as well as smoldering low-temperature regions, leading to heterogeneity in properties. Defining a continuum of CI instead of temperature in lab charcoals will help clarify these field issues, and further work should be done to assess the effect that oxygen availability has on this parameter.

■ ASSOCIATED CONTENT

Supporting Information

The Supporting Information is available free of charge on the ACS Publications website at DOI: 10.1021/acs.est.5b03087.

Tables showing biomass characterization, selected peak area ratios for pyrolyzed samples, and definition and values for all parameters used in the Matlab grassland and forest fire simulations. Figures showing the percent carbon and nitrogen of the original biomass in samples, ATR-FTIR spectra of all samples, and model results for total N and δ^{15}N in soil and plant pools. Additional details on the FTIR analysis and nitrogen mass-balance model. (PDF)

■ AUTHOR INFORMATION

Corresponding Author

*Phone: (361)215-4963; e-mail: Lacey.a.Pyle@rice.edu.

Notes

The authors declare no competing financial interest.

■ ACKNOWLEDGMENTS

We thank Chase Lecroy for assisting with charcoal production operations and the Rice Shared Equipment Authority for providing access to the ATR-FTIR. We acknowledge support from NSF grants EAR-0949337 and EAR-0911685.

■ REFERENCES

(1) Schmidt, M. W. I.; Noack, A. G. Black carbon in soils and sediments: Analysis, distribution, implications, and current challenges. *Global Biogeochem. Cycles* **2000**, *14* (3), 777−793.

(2) Keiluweit, M.; Nico, P. S.; Johnson, M. G.; Kleber, M. Dynamic Molecular Structure of Plant Biomass-Derived Black Carbon (Biochar). *Environ. Sci. Technol.* **2010**, *44* (4), 1247−1253.

(3) Masiello, C. New directions in black carbon organic geochemistry. *Mar. Chem.* **2004**, *92* (1−4), 201−213.

(4) Novak, J.; Busscher, W.; Laird, D.; Ahmedna, M.; Watts, D. W.; Niandou, M. A. S. Impact of biochar amendment on fertility of a southeastern coastal plain soil. *Soil Sci.* **2009**, *174* (2), 105−112.

(5) Kuhlbusch, T. A. J.; Crutzen, P. J. Toward a global estimate of black carbon in residues of vegetation fires representing a sink of atmospheric CO_2 and a source of O_2. *Global Biogeochem. Cycles* **1995**, *9* (4), 491−501.

(6) Baldock, J.; Smernik, R. Chemical composition and bioavailability of thermally altered Pinus resinosa(Red pine) wood. *Org. Geochem.* **2002**, *33* (9), 1093−1109.

(7) Lehmann, J. A handful of carbon. *Nature* **2007**, *447*, 143−144.

(8) Hockaday, W. C.; Grannas, A. M.; Kim, S.; Hatcher, P. G. The transformation and mobility of charcoal in a fire-impacted watershed. *Geochim. Cosmochim. Acta* **2007**, *71* (14), 3432−3445.

(9) Middelburg, J. J.; Nieuwenhuize, J.; Van Breugel, P. Black carbon in marine sediments. *Mar. Chem.* **1999**, *65* (3−4), 245−252.

(10) Wiedemeier, D. B.; Abiven, S.; Hockaday, W. C.; Keiluweit, M.; Kleber, M.; Masiello, C. A.; McBeath, A. V.; Nico, P. S.; Pyle, L. A.; Schneider, M. P. W.; et al. Aromaticity and degree of aromatic condensation of char. *Org. Geochem.* **2014**, *78*, 135−143.
(11) Wurster, C. M.; Saiz, G.; Schneider, M. P. W.; Schmidt, M. W. I.; Bird, M. I. Quantifying pyrogenic carbon from thermosequences of wood and grass using hydrogen pyrolysis. *Org. Geochem.* **2013**, *62*, 28−32.
(12) Mcbeath, A. V.; Smernik, R. J.; Schneider, M. P. W.; Schmidt, M. W. I.; Plant, E. L. Determination of the aromaticity and the degree of aromatic condensation of a thermosequence of wood charcoal using NMR. *Org. Geochem.* **2011**, *42* (10), 1194−1202.
(13) Czimczik, C.; Preston, C.; Schmidt, M.; Werner, R. A.; Schulze, E.-D. Effects of charring on mass, organic carbon, and stable carbon isotope composition of wood. *Org. Geochem.* **2002**, *33*, 1207−1223.
(14) Schneider, M. P. W.; Smittenberg, R. H.; Dittmar, T.; Schmidt, M. W. I. Comparison of gas with liquid chromatography for the determination of benzenepolycarboxylic acids as molecular tracers of black carbon. *Org. Geochem.* **2011**, *42* (3), 275−282.
(15) Bird, M. I.; Ascough, P. L. Isotopes in pyrogenic carbon: A review. *Org. Geochem.* **2012**, *42* (12), 1529−1539.
(16) Wójtowicz, M. The fate of nitrogen functionalities in coal during pyrolysis and combustion. *Fuel* **1995**, *74* (4), 507−516.
(17) Pels, J. R.; Kapteijn, F.; Moulijn, J. A.; Zhu, Q.; Thomas, K. M. Evolution of nitrogen functionalities in carbonaceous materials during pyrolysis. *Carbon* **1995**, *33* (11), 1641−1653.
(18) Almendros, G.; Knicker, H.; González-Vila, F. Rearrangement of carbon and nitrogen forms in peat after progressive thermal oxidation as determined by solid-state ^{13}C-and ^{15}N-NMR. *Org. Geochem.* **2003**, *34* (11), 1559−1568.
(19) Bogaard, A.; Heaton, T. H. E.; Poulton, P.; Merbach, I. The impact of manuring on nitrogen isotope ratios in cereals: archaeological implications for reconstruction of diet and crop management practices. *J. Archaeol. Sci.* **2007**, *34* (3), 335−343.
(20) Fraser, R.; Bogaard, A.; Charles, M. Assessing natural variation and the effects of charring, burial and pre-treatment on the stable carbon and nitrogen isotope values of archaeobotanical cereals and pulses. *J. Archaeol. Sci.* **2013**, *40* (12), 4754−4766.
(21) Aguilera, M.; Araus, J. L.; Voltas, J.; Rodriguez-Ariza, M. O.; Molina, F.; Rovira, N.; Buxo, R.; Ferrio, J. P. Stable carbon and nitrogen isotopes and quality traits of fossil cereal grains provide clues on sustainability at the beginnings of Mediterranean agriculture. *Rapid Commun. Mass Spectrom.* **2008**, *22* (11), 1653−1663.
(22) Huber, E.; Bell, T. L.; Adams, M. A. Combustion influences on natural abundance nitrogen isotope ratio in soil and plants following a wildfire in a sub-alpine ecosystem. *Oecologia* **2013**, *173*, 1063−1074.
(23) Peng, X.; Ye, L.; Wang, C.; Zhou, H.; Sun, B. Temperature-and duration-dependent rice straw-derived biochar: Characteristics and its effects on soil properties of an Ultisol in southern China. *Soil Tillage Res.* **2011**, *112*, 159−166.
(24) Sun, H.; Hockaday, W. C.; Masiello, C. A.; Zygourakis, K. Multiple Controls on the Chemical and Physical Structure of Biochars. *Ind. Eng. Chem. Res.* **2012**, *51*, 3587−3597.
(25) Ronsse, F.; van Hecke, S.; Dickinson, D.; Prins, W. Production and characterization of slow pyrolysis biochar: influence of feedstock type and pyrolysis conditions. *GCB Bioenergy* **2013**, *5*, 104−115.
(26) Wang, Y.; Hu, Y.; Zhao, X.; Wang, S.; Xing, G. Comparisons of Biochar Properties from Wood Material and Crop Residues at Different Temperatures and Residence Times. *Energy Fuels* **2013**, *27*, 5890−5899.
(27) Harvey, O.; Kuo, L.; Zimmerman, A. R.; Louchouarn, P.; Amonette, J. E.; Herbert, B. E. An index-based approach to assessing recalcitrance and soil carbon sequestration potential of engineered black carbons (biochars). *Environ. Sci. Technol.* **2012**, *46*, 1415−1421.
(28) Zimmerman, A. Abiotic and microbial oxidation of laboratory-produced black carbon (biochar). *Environ. Sci. Technol.* **2010**, *44* (4), 1295−1301.
(29) Sun, H.; Zhou, Z. Impacts of charcoal characteristics on sorption of polycyclic aromatic hydrocarbons. *Chemosphere* **2008**, *71* (11), 2113−2120.
(30) Chen, B.; Chen, Z. Sorption of naphthalene and 1-naphthol by biochars of orange peels with different pyrolytic temperatures. *Chemosphere* **2009**, *76* (1), 127−133.
(31) Fang, Y.; Singh, B.; Singh, B. P.; Krull, E. Biochar carbon stability in four contrasting soils. *Eur. J. Soil Sci.* **2014**, *65* (1), 60−71.
(32) Antal, M. J. Effects of reactor severity on the gas-phase pyrolysis of cellulose- and kraft lignin-derived volatile matter. *Ind. Eng. Chem. Prod. Res. Dev.* **1983**, *22* (2), 366−375.
(33) Company, U. S. S. *Min-u-sil ® 40 Product Data*.
(34) Scheirs, J.; Camino, G.; Tumiatti, W. Overview of water evolution during the thermal degradation of cellulose. *Eur. Polym. J.* **2001**, *37* (5), 933−942.
(35) Yang, H.; Yan, R.; Chen, H.; Lee, D. H.; Zheng, C. Characteristics of hemicellulose, cellulose and lignin pyrolysis. *Fuel* **2007**, *86* (12−13), 1781−1788.
(36) Coplen, T. Reporting of stable hydrogen, carbon, and oxygen isotopic abundances. *Pure Appl. Chem.* **1994**, *66* (2), 273−276.
(37) Mariotti, A. Atmospheric nitrogen is a reliable standard for natural ^{15}N abundance measurements. *Nature* **1983**, *303*, 685−687.
(38) Wojdyr, M. Fityk 0.9.8. *J. Appl. Crystallogr.* **2010**, *43*, 1126−1128.
(39) Brenner, D. L.; Amundson, R.; Baisden, W. T.; Kendall, C.; Harden, J. Soil N and ^{15}N variation with time in a California annual grassland ecosystem. *Geochim. Cosmochim. Acta* **2001**, *65* (22), 4171−4186.
(40) Sun, Y.; Cheng, J. Hydrolysis of lignocellulosic materials for ethanol production: A review. *Bioresour. Technol.* **2002**, *83* (1), 1−11.
(41) McRae, C.; Love, G. D.; Murray, I. P.; Snape, C. E.; Fallick, A. E. Potential of gas chromatography isotope ratio mass spectrometry to source polycyclic aromatic hydrocarbon emissions. *Anal. Commun.* **1996**, *33* (9), 331.
(42) Song, J.; Huang, W.; Peng, P. Stability and carbon isotope changes of soot and char materials during thermal oxidation: Implication for quantification and source appointment. *Chem. Geol.* **2012**, *330−331*, 159−164.
(43) Pessenda, L. C. R.; Ledru, M. P.; Gouveia, S. E. M.; Aravena, R.; Ribeiro, A. S.; Bendassolli, J. A.; Boulet, R. Holocene palaeoenvironmental reconstruction in northeastern Brazil inferred from pollen, charcoal and carbon isotope records. *Holocene* **2005**, *15* (6), 812−820.
(44) Hall, G.; Woodborne, S.; Scholes, M. Stable carbon isotope ratios from archaeological charcoal as palaeoenvironmental indicators. *Chem. Geol.* **2008**, *247* (3−4), 384−400.
(45) Knicker, H. Black nitrogen" - an important fraction in determining the recalcitrance of charcoal. *Org. Geochem.* **2010**, *41*, 947−950.
(46) Hilscher, A.; Heister, K.; Siewert, C.; Knicker, H. Mineralisation and structural changes during the initial phase of microbial degradation of pyrogenic plant residues in soil. *Org. Geochem.* **2009**, *40* (3), 332−342.
(47) Hobbie, E.; Högberg, P. Nitrogen isotopes link mycorrhizal fungi and plants to nitrogen dynamics. *New Phytol.* **2012**, *196* (2), 367−382.
(48) Kinney, T. J.; Masiello, C. A.; Dugan, B.; Hockaday, W. C.; Dean, M. R.; Zygourakis, K.; Barnes, R. T. Hydrologic properties of biochars produced at different temperatures. *Biomass Bioenergy* **2012**, *41*, 34−43.
(49) Mukome, F. N. D.; Six, J.; Parikh, S. J. The effects of walnut shell and wood feedstock biochar amendments on greenhouse gas emissions from a fertile soil. *Geoderma* **2013**, *200−201*, 90−98.
(50) Guo, Y.; Bustin, R. M. FTIR spectroscopy and reflectance of modern charcoals and fungal decayed woods: implications for studies of inertinite in coals. *Int. J. Coal Geol.* **1998**, *37* (1−2), 29−53.
(51) Pastorova, I.; Botto, R. E.; Arisz, P. W.; Boon, J. J. Cellulose char structure: A combined analytical Py-GC-MS, FTIR, and NMR study. *Carbohydr. Res.* **1994**, *262* (1), 27−47.

DOI: 10.1021/acs.est.5b03087
Environ. Sci. Technol. 2015, 49, 14057−14064

(52) Högberg, P. Tansley Review No. 95 ^{15}N natural abundance in soil-plant systems. *New Phytol.* **1997**, *137* (2), 179−203.
(53) Grogan, P.; Burns, T. D.; Chapin III, F. S. Fire effects on ecosystem nitrogen cycling in a Californian bishop pine forest. *Oecologia* **2000**, *122* (4), 537−544.
(54) Saito, L.; Miller, W. W.; Johnson, D. W.; Qualls, R. G.; Provencher, L.; Carroll, E.; Szameitat, P. Fire effects on stable isotopes in a Sierran forested watershed. *J. Environ. Qual.* **2007**, *36* (1), 91−100.
(55) Wolf, M.; Lehndorff, E.; Wiesenberg, G. L. B.; Stockhausen, M.; Schwark, L.; Amelung, W. Towards reconstruction of past fire regimes from geochemical analysis of charcoal. *Org. Geochem.* **2013**, *55*, 11−21.
(56) Schafer, J. L.; Mack, M. C. Short-term effects of fire on soil and plant nutrients in palmetto flatwoods. *Plant Soil* **2010**, *334* (1−2), 433−447.
(57) de la Rosa, J.; Knicker, H. Bioavailability of N released from N-rich pyrogenic organic matter: an incubation study. *Soil Biol. Biochem.* **2011**, *43* (12), 2368−2373.
(58) Hilscher, A.; Knicker, H. Carbon and nitrogen degradation on molecular scale of grass-derived pyrogenic organic material during 28 months of incubation in soil. *Soil Biol. Biochem.* **2011**, *43* (2), 261−270.
(59) Sotirchos, S. V.; Amundson, N. R. Diffusion and reaction in a char particle and in the surrounding gas phase. A Continuous Model. *Ind. Eng. Chem. Fundam.* **1984**, *23* (2), 191−201.
(60) Hobbie, E. A.; Ouimette, A. P. Controls of nitrogen isotope patterns in soil profiles. *Biogeochemistry* **2009**, *95* (2−3), 355−371.
(61) Hobbie, E.; Macko, S.; Shugart, H. Insights into nitrogen and carbon dynamics of ectomycorrhizal and saprotrophic fungi from isotopic evidence. *Oecologia* **1999**, *118* (3), 353−360.
(62) Högberg, P.; Högbom, L.; Schinkel, H.; Högberg, M.; Johannisson, C.; Wallmark, H. ^{15}N abundance of surface soils, roots and mycorrhizas in profiles of European forest soils. *Oecologia* **1996**, *108* (2), 207−214.
(63) Forbes, M. S.; Raison, R. J.; Skjemstad, J. O. Formation, transformation and transport of black carbon (charcoal) in terrestrial and aquatic ecosystems. *Sci. Total Environ.* **2006**, *370* (1), 190−206.
(64) Dai, X.; Boutton, T. W.; Glaser, B.; Ansley, R. J.; Zech, W. Black carbon in a temperate mixed-grass savanna. *Soil Biol. Biochem.* **2005**, *37* (10), 1879−1881.
(65) Toma, Y.; Fernandez, F.; Nishiwaki, A.; Yamada, T.; Bollero, G.; Stewart, J. R. Aboveground plant biomass, carbon, and nitrogen dynamics before and after burning in a seminatural grassland of *Miscanthus sinensis* in Kumamoto, Japan. *GCB Bioenergy* **2010**, *2*, 52−62.
(66) Rau, B. M.; Tausch, R.; Reiner, A.; Johnson, D. W.; Chambers, J. C.; Blank, R. R.; Lucchesi, A. Influence of Prescribed Fire on Ecosystem Biomass, Carbon, and Nitrogen in a Pinyon Juniper Woodland. *Rangel. Ecol. Manag.* **2010**, *63* (2), 197−202.
(67) Hubbard, R. M.; Vose, J. M.; Clinton, B. D.; Elliott, K. J.; Knoepp, J. D. Stand restoration burning in oak-pine forests in the southern Appalachians: Effects on aboveground biomass and carbon and nitrogen cycling. *For. Ecol. Manage.* **2004**, *190*, 311−321.
(68) Cao, Z. H.; Ding, J. L.; Hu, Z. Y.; Knicker, H.; Kögel-Knabner, I.; Yang, L. Z.; Yin, R.; Lin, X. G.; Dong, Y. H.; et al. Ancient paddy soils from the Neolithic age in China's Yangtze River Delta. *Naturwissenschaften* **2006**, *93* (5), 232−236.

DOI: 10.1021/acs.est.5b03087
Environ. Sci. Technol. 2015, 49, 14057−14064

Supporting Information

"Chemical and isotopic thresholds in charring: implications for the interpretation of charcoal mass and isotopic data"

Authors: Lacey A. Pyle*, William C. Hockaday, Thomas Boutton, Kyriacos Zygourakis, Timothy J. Kinney, Caroline A. Masiello

Supporting information (7 pages) contains further FTIR analysis and mass balance model description. Supplemental Table 1 is starting biomass values for charred products, Supplemental Figure 1 and 2 are chemical char characterizations grouped by peak temperature, Supplemental Figure 3 is some representative FTIR spectra, Supplemental Table 2 contains FTIR peak ratios, Supplemental Tables 3 and 4 are model parameters, and Supplemental Figures 4 and 5 are the results of our model runs in two different ecosystems and under two different fire regimes.

Supporting Information

Supplemental Table 1. Biomass characterization					
Biomass	$\delta^{15}N$	%N	$\delta^{13}C$	%C	C:N
Apple Wood	2.87	0.29	-27.39	46.88	161.66
Mesquite Wood	1.99	0.79	-26.16	46.98	59.47
Cocklebur	4.49	0.95	-27.84	39.86	41.96
Corn Stover	-1.08	0.63	-12.75	44.04	69.91

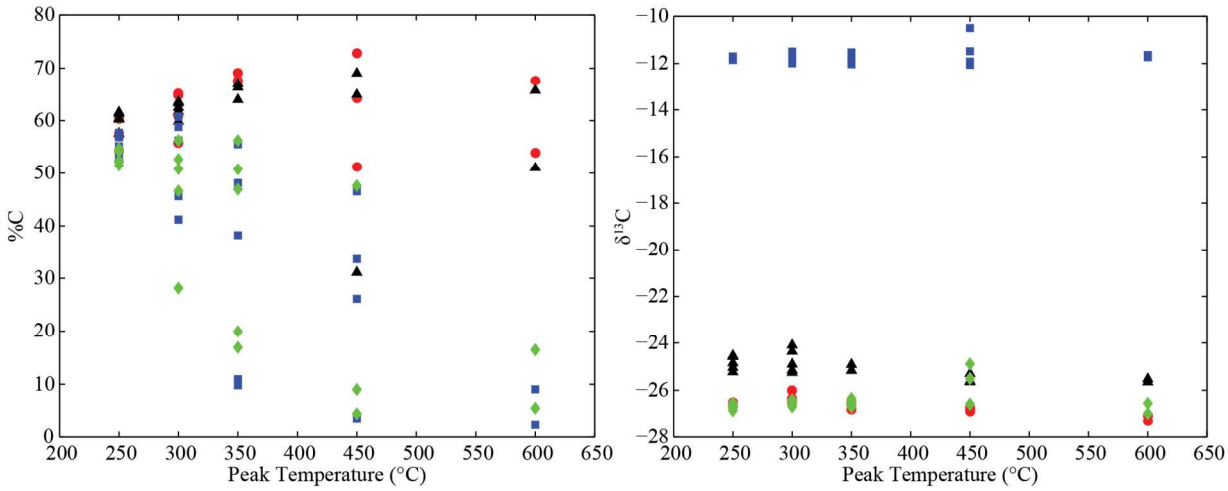

Supplemental Figure 1. A) Percent carbon of original biomass remaining in pyrolyzed samples. B) Carbon isotope values of pyrolyzed samples. Apple char samples are represented by circles, corn char by squares, cocklebur char by diamonds and mesquite char by triangles.

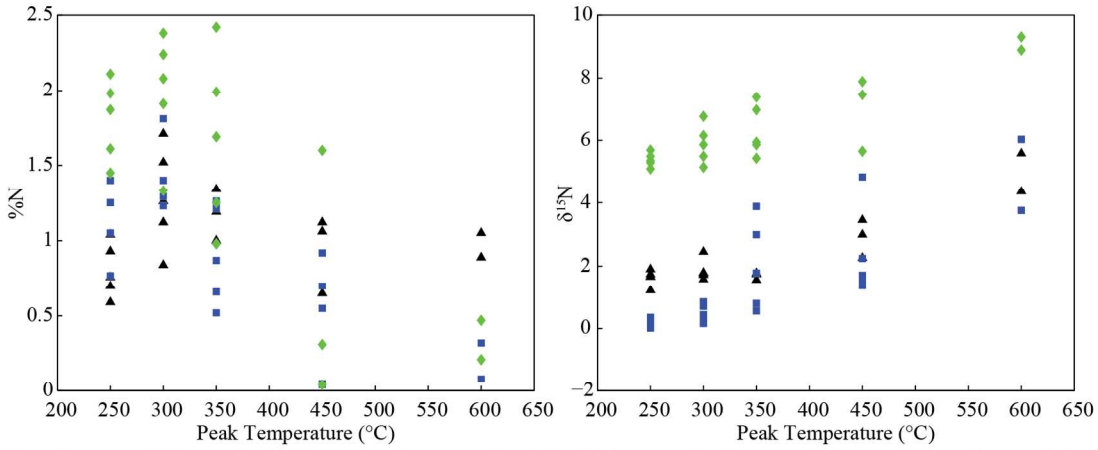

Supplemental Figure 2. A) Percent nitrogen of original biomass in the remaining pyrolyzed material. B) Nitrogen isotope values of each pyrolyzed sample. Corn char samples are represented by squares, cocklebur char by diamonds and mesquite char by triangles. (For apple char, very low initial N concentrations limited detection of changes in %N, and it is excluded from N figures.)

FTIR Analysis

Changes in the charcoal FTIR spectra across the CI gradient show a loss of the original biomass complexity as charcoals progress to larger, more rigid aromatic structures (Figure 7). This spectral charring transition is consistent with previous studies(Pastorova et al 1994; Keiluweit et al 2010; Kinney et al 2012). All spectra are dominated by peaks at 1056 cm-1, 1600 cm-1, and 1700 cm-1 and additionally have a broad water peak between 2500-3700 cm-1 (Figure 7). Aliphatic peaks occurring between 3000-2800cm-1 are present at lower CI and disappear at higher intensities(Pastorova et al 1994; Guo and Bustin 1998; Keiluweit et al 2010; Hobbie and Högberg 2012; Kinney et al 2012). A peak at 1311 cm-1 attributed to aliphatic -CH2- deformations initially increases as CI increases, but begins to disappear later, a behavior which agrees with the charcoal FTIR literature(Guo and Bustin 1998). Using this aliphatic peak in a ratio compared to the aromatic peak at 1600 cm-1 results in a decreasing trend with CI, indicating more charred products(Guo and Bustin 1998; Mukome et al 2013).

Charcoal chemistry becomes increasingly aromatic with a coinciding decrease in aliphatics along our CI gradient (Supplemental Figure 1). Additionally a peak at 1160 cm-1, which could correspond to cellulose derived charring products, increases linearly with CI (Keiluweit et al 2010). Although the large method-derived silica peak prevents definitive confirmation that carbohydrates are disappearing because deconvolution of the two peaks was not possible, the increasing aromaticity of the samples as well as the appearance of aromatic C-H bonds and cellulose-derived charring products does indicate increasingly charred products, implying carbohydrates are also being consumed.

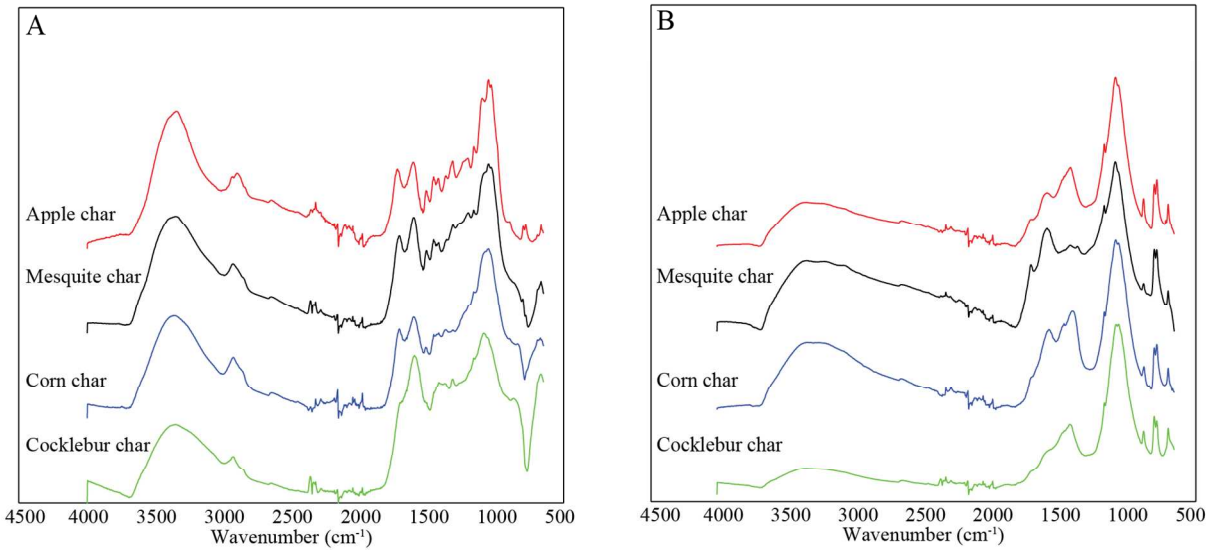

Supplemental Figure 3. ATR-FTIR spectra of all charcoal samples within this study at (A) low intensity and (B) high intensity.

Supplemental Table 2. Selected peak area ratios for pyrolyzed samples (Apple = A, Mesquite = M, Cocklebur = X, Corn = C)													
Peak Area Ratios		1600/1700				780-885/1600				2800-3000/1600			
Feedstock		A	M	X	C	A	M	X	C	A	M	X	C
Charring Intensities	1.7E+06	0.09	0.06	0.06	0.25	0.15	0.82	0.82	0.02	1.00	1.00	1.00	0.64
	1.8E+06	0.12	0.16	0.16	0.40	0.28	0.19	0.19	0.03	0.17	0.10	0.10	0.16
	2.5E+06	0.32	0.22	0.22	0.45	0.14	0.26	0.26	0.02	0.29	0.06	0.06	0.04
	2.5E+06	0.09	0.10	0.10	0.29	0.12	0.58	0.58	0.02	0.66	0.33	0.33	0.39
	2.9E+06	0.12	0.14	0.14	0.45	0.35	1.00	1.00	0.04	0.11	0.13	0.13	0.11
	3.4E+06	0.10	0.06	0.06	0.31	0.10	0.17	0.17	0.01	0.29	0.28	0.28	0.30
	3.8E+06	0.22	0.17	0.17	0.62	0.06	0.55	0.55	0.05	0.11	0.06	0.06	0.04
	3.9E+06	0.21	0.14	0.14	0.50	0.09	0.35	0.35	0.03	0.20	0.09	0.09	0.11
	4.2E+06	0.10	0.07	0.07	0.26	0.25	0.18	0.18	0.04	0.16	0.18	0.18	0.26
	4.2E+06	0.33	0.23	0.23	0.57	0.10	0.34	0.34	0.03	0.05	0.05	0.05	0.01
	4.9E+06	0.26	0.34	0.34	0.35	0.06	0.70	0.70	0.10	0.06	0.04	0.04	0.09
	5.0E+06	0.26	0.13	0.13	0.46	0.06	0.29	0.29	0.08	0.26	0.07	0.07	0.08
	5.0E+06	0.11	0.10	0.10	0.26	0.16	0.29	0.29	0.05	0.15	0.13	0.13	0.22
	5.8E+06	0.31	0.29	0.29	0.47	0.54	0.68	0.68	0.10	0.07	0.04	0.04	0.02
	6.0E+06	0.32	0.11	0.11	0.47	0.39	0.85	0.85	0.08	0.38	0.12	0.12	0.07
	6.2E+06	0.27			0.19	0.87			0.50	0.05			0.26
	7.0E+06	1.00	0.63	0.63	1.00	0.37	0.92	0.92	0.06	0.02	0.02	0.02	0.05
	7.4E+06	0.28	0.32	0.32	0.43	1.00	0.66	0.66	0.13	0.06	0.04	0.04	0.02
	7.4E+06	0.34			0.26	0.14			0.64	0.05			0.40
	8.7E+06				0.38				1.00				0.32
	8.9E+06				0.35				0.44				0.42
	1.0E+07				0.29				0.52				1.00
	1.0E+07	0.94	1.00	1.00	0.35	0.40	0.58	0.58	0.56	0.01	0.01	0.01	0.19

Nitrogen Mass Balance Model

The model in Brenner et al, 2001 is a simple mass balance for total nitrogen and nitrogen isotopes in a coupled soil and plant system. We recreated this model but also added a perturbation in the form of a fire every 10 years in order to show that the black nitrogen produced in a fire makes a significant impact on soil nitrogen isotopes. We used parameters for a grassland and a boreal forest, shown in supplemental Tables 3 and 4, to produce Supplemental Figures 4 and 5. The fire model simply removes a portion of aboveground biomass to the

atmosphere as gaseous losses (k_{exc}) and then a smaller portion is transferred from the plant N pool to the soil N pool (k_c) with the associated fractionation factor found through our laboratory work (α_c). It is important to note that in the simulations represented below, the ~4‰ fractionation in both grasslands and forests is driven mainly by the large losses directly to the atmosphere from combustion of plant material. However, when we simulated with just char production alone (an unrealistic scenario not pictured here) we still found a 1‰ increase in soil N isotopes.

Supplemental Table 3. Definition and values of all parameters used in Matlab grassland fire simulation		
Parameter	Description	Value Used
R_{ex}	15N/14N of atmospheric inputs	0.0036765
α_{ex}	Soil to environment N fractionation factor	0.995
α_p	Soil to plant N fractionation factor	0.990
I_{ex}	Atmospheric N deposition	10
k_{ex}	Soil N loss constant (soil to environment)	0.002
k_s	Plant N loss constant (plant to soil)	0.1
k_p	Soil N loss constant (soil to plants)	0.02
I_{fix}	N fixation	2.3
k_c	plant to char loss constant	0.027
α_c	plant to char N fractionation factor	1.000996016
k_{exc}	plant to environment loss after fire	0.93

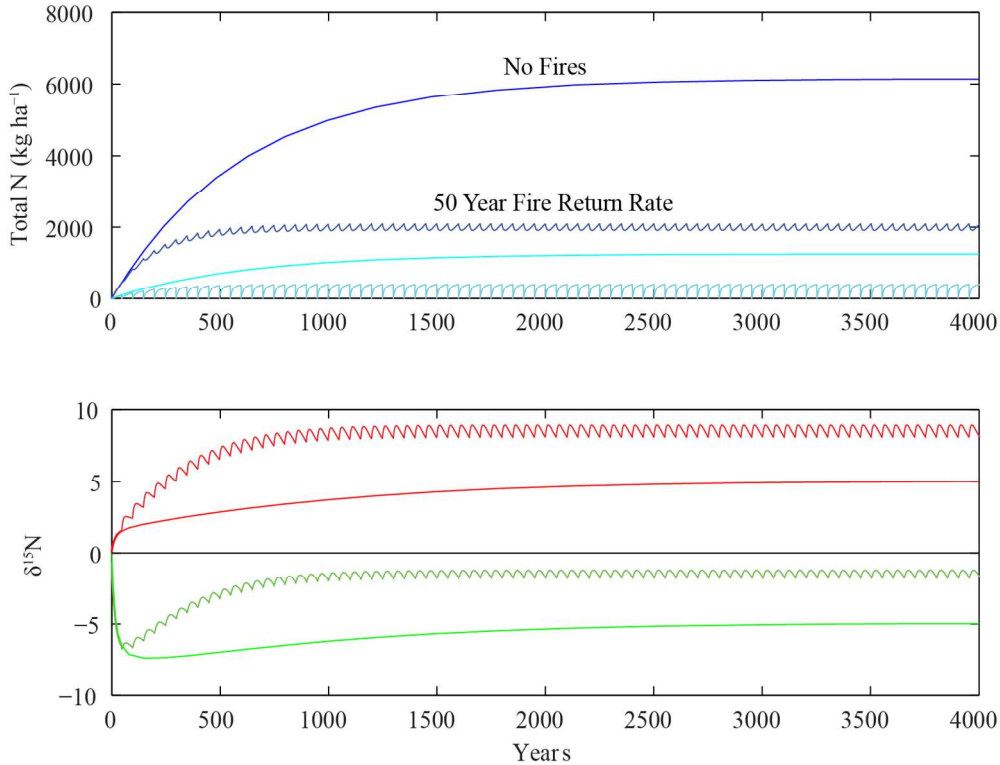

Supplemental Figure 4. Model results for (A) total N and (B) $\delta^{15}N$ in the soil and plant pools from a control grassland with and without fire disturbance. The blue and red lines represent the soil nitrogen pool and the cyan and green lines represent the plant pool.

Supplemental Table 4. Definition and values of all parameters used in Matlab forest fire simulation		
Parameter	Description	Value Used
R_{ex}	15N/14N of atmospheric inputs	0.0036765
α_{ex}	Soil to environment N fractionation factor	0.995
α_p	Soil to plant N fractionation factor	0.990
I_{ex}	Atmospheric N deposition	12.5
k_{ex}	Soil N loss constant (soil to environment)	0.002
k_s	Plant N loss constant (plant to soil)	0.1
k_p	Soil N loss constant (soil to plants)	0.04
I_{fix}	N fixation	6.5
k_c	plant to char loss constant	0.0174
α_c	plant to char N fractionation factor	1.002401008
k_{exc}	plant to environment loss after fire	0.58

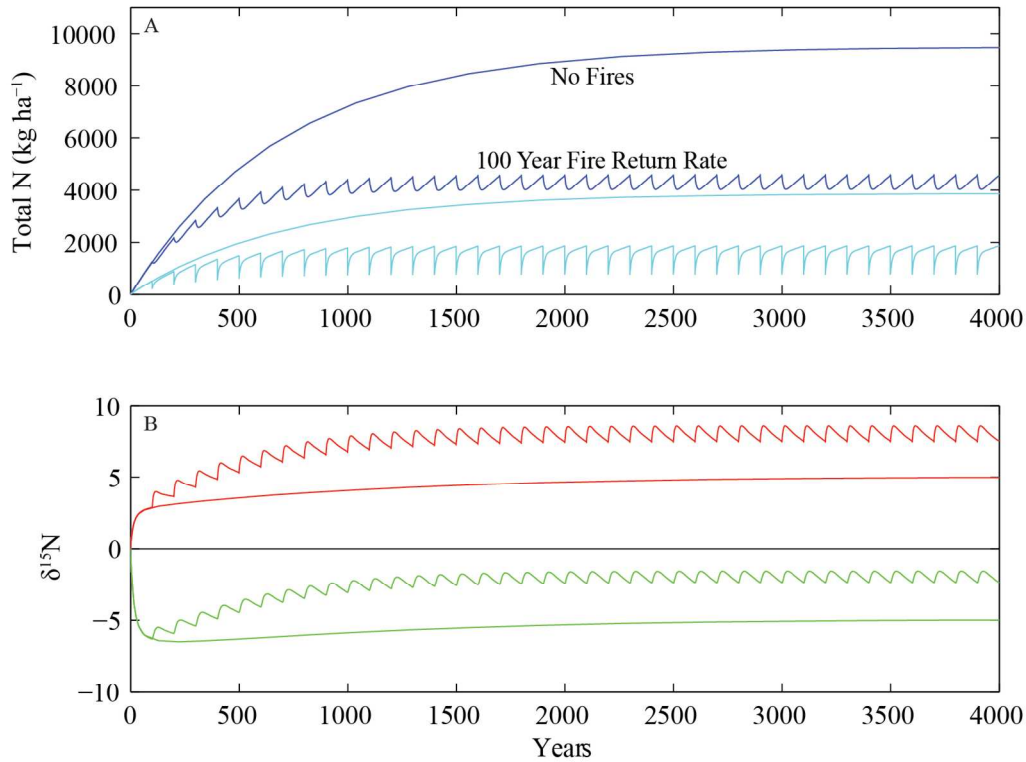

Supplemental Figure 5. Model results for (A) total N and (B) $\delta^{15}N$ in the soil and plant pools from a control grassland with and without fire disturbance. The blue and red lines represent the soil nitrogen pool and the cyan and green lines represent the plant pool.